

Influence of the Grafting Density on the Self-Assembly in Poly(phenyleneethynylene)-*g*-poly(3-hexylthiophene) Graft Copolymers

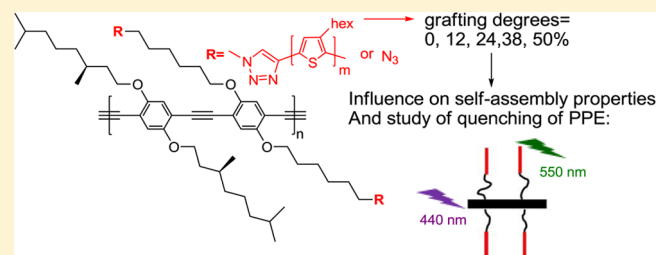
Joost Steverlynck,[†] Julien De Winter,[‡] Pascal Gerbaux,[‡] Roberto Lazzaroni,[§] Philippe Leclère,[§] and Guy Koeckelberghs^{*,†}

[†]Laboratory for Polymer Synthesis, KU Leuven, Celestijnenlaan 200F, B-3001 Heverlee, Belgium

[‡]Organic Synthesis and Mass Spectrometry Laboratory, Interdisciplinary Center for Mass Spectrometry, and [§]Laboratory for Chemistry of Novel Materials, Center for Innovation and Research in Materials and Polymers (CIRMAP), University of Mons-UMONS, 7000 Mons, Belgium

Supporting Information

ABSTRACT: Conjugated graft copolymers consisting of a chiral poly(phenyleneethynylene) (PPE) backbone and poly(3-hexylthiophene) side chains (P3HT) with different grafting degrees were synthesized. While PPE was prepared by classical Sonogashira couplings, the end-functionalized P3HT was prepared by a controlled Kumada catalyst transfer polycondensation (KCTP) allowing the installation of an acetylene end group. After some postpolymerization reactions on the PPE to introduce azide groups, the P3HT was clicked to the PPE through the CuAAC coupling reaction. Subsequently, the (chiral) self-assembly of these materials was studied by means of UV-vis and CD spectroscopy, AFM, and DSC. Finally, fluorescence spectroscopy is used to study the quenching of the PPE fluorescence by P3HT.



INTRODUCTION

For nonconjugated polymers, extensive research has already been performed in the field of graft copolymers. Progress in the domain of controlled polymerizations allowed the production of well-defined molecular brushes.¹ These structures show some unusual properties that are not observed for their linear counterparts, making new applications possible. These features include their wormlike behavior and compact molecular dimension.² A lot of parameters like the length of the backbone and side chains as well as the grafting density can be optimized to obtain the desired properties. By variation of these parameters, different precisely defined nanostructures can be obtained which can act as template for inorganic nanostructures or as very stable micelles that can be used as drug carriers.² This type of polymers can also lead to super soft elastomers and photonic materials.²

Conjugated polymers (CPs) have been investigated for decades, as they show some unique properties and applications compared with their nonconjugated counterparts. Especially their optoelectronic properties together with their solution processability make them very useful for implementation as active material into low-cost electronics like organic photovoltaics (OPVs), organic field effect transistors (OFETs), and organic light-emitting diodes (OLEDs).^{3–6}

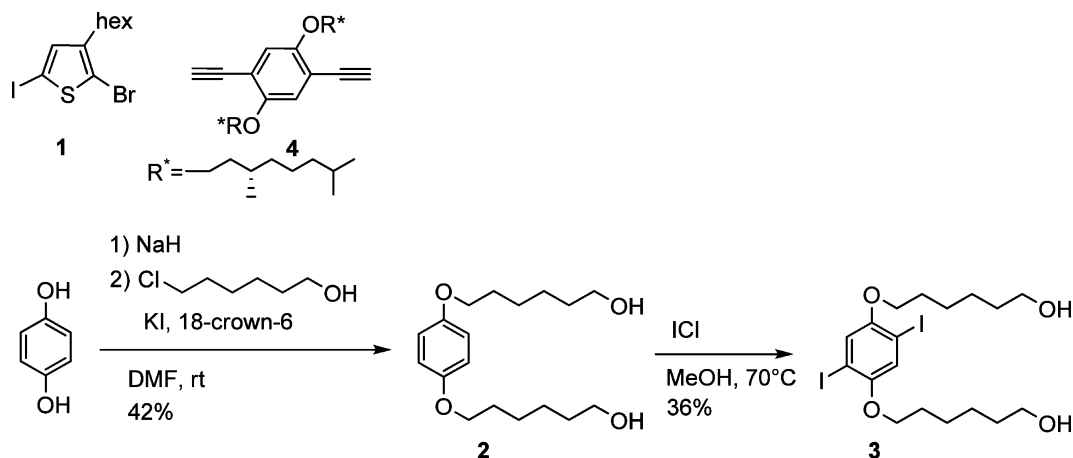
Despite the fact that graft copolymers can show a unique behavior compared to the linear analogues, up until now, in the field of conjugated polymers the focus mainly has been on the

synthesis of linear structures. These include homopolymers and different types of (block) copolymers. In recent years some progress has been made in the synthesis of conjugated polymers with a controllable degree of branching.⁷ The field of graft copolymers is even less explored, mainly due to synthetic challenges. Nonetheless, these materials offer a whole new range of possibilities, like production of solar cells with broadband absorbance and the study of energy transfer processes.^{8,9} In comparison to block copolymers the ratio between the polymers can be more effectively tuned. The synthesis of conjugated graft copolymers has only been reported for two systems and this by the “grafting from” and “graft through” methods.^{10,11} However, chirality has never been introduced, although it offers a lot of opportunities for both characterization of the material and its properties. For instance, circular dichroism (CD) can be observed in chiral conjugated polymers and used to explore the supramolecular structure of these materials.^{12,13} Also, the influence of the grafting density in CPs has never been investigated, although it can be assumed that it severely affects the self-assembly and, hence, the properties. In this report, we describe the synthesis, (chiral) self-assembly, and emission characteristics of a series of grafted conjugated polymers consisting of a PPE backbone with P3HT

Received: August 19, 2015

Revised: November 25, 2015

Scheme 1. Structure and Synthesis of the Monomers



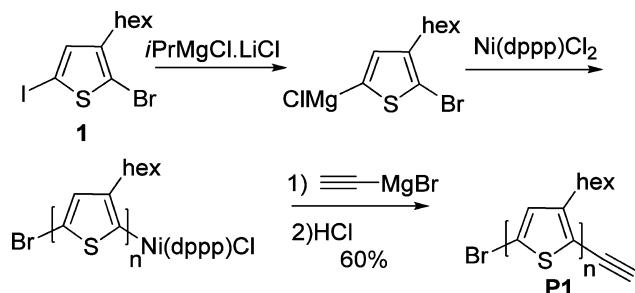
side chains and investigate the influence of the different grafting density on these properties.

RESULTS AND DISCUSSION

Monomer Synthesis. While the monomer **1** for the synthesis of P3HT is commercial, the chiral monomer **4** was synthesized according to literature procedures.⁷ Monomer **3** was obtained by alkylation of hydroquinone with 6-chlorohexanol, followed by iodination with ICl (Scheme 1).^{14–18} Methods using NIS and KIO₃ with I₂ in acidic medium lead to formation of side products. A chiral side chain was used, since it allows the study of the self-assembly with chiral techniques, e.g., CD.

Polymer Synthesis. Acetylene end-capped P3HT (**P1**) was obtained by polymerization of 2-chloromagnesio-5-bromohexylthiophene, *in situ* prepared by a modified GRIM reaction, using the KCTP (Scheme 2). After 15 min of polymerization the end-capper was added in excess.^{19–22} After another 15 min the reaction was terminated by adding acid.

Scheme 2. Synthesis of Polymer P1



Analysis of the MALDI-ToF spectra indicates a mixture of mainly Br/acetylene-terminated polymers and another series of polymers, attributed to dialkyne P3HT, as minor product.^{23,24} Based on the MALDI analyses, this second distribution should represent less than 25% of contamination (see Supporting Information, S9).

In the ¹H NMR spectrum, next to the signal for the internal α -CH₂, there is a clear triplet signal corresponding to a α -CH₂ at a terminal unit with a bromine end (Figure 1).²⁵ Since also some dicapped polymers are present (MALDI-ToF), an exact determination of the DP by ¹H NMR spectroscopy is impossible.

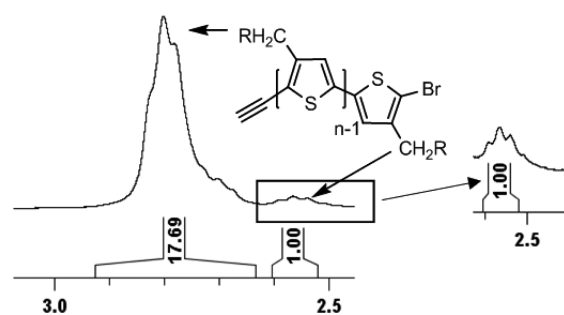


Figure 1. ¹H NMR signal of α -CH₂ of P3HT (**P1**).

GPC calibrated against polystyrene standards results in an \bar{M}_n value of 4.4 kg/mol and a dispersity of 1.2, which is in line with the expected living KCTP. The \bar{M}_n value corresponds to 26 units. This is higher than expected but can be explained by the fact that this technique overestimates the molar mass of P3HT.^{26,27} When using the correction factor of 1.3, determined by Seferos et al., we obtain a degree of polymerization of 20.²⁷ This is close to the targeted \bar{M}_n value of 18.

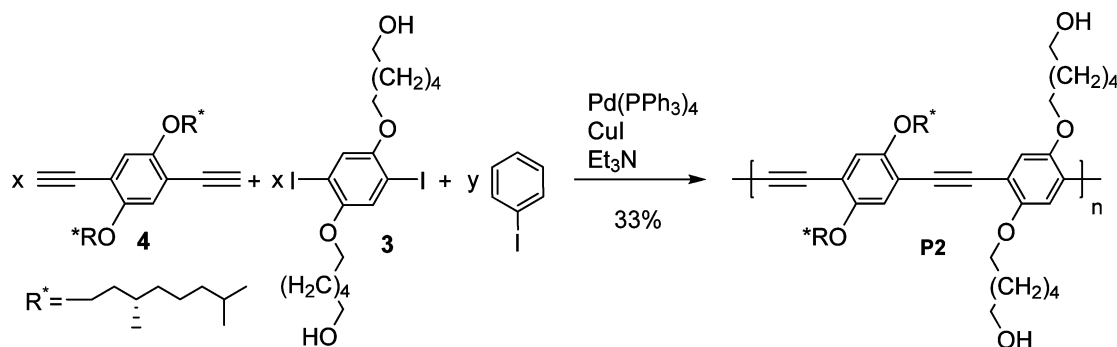
The PPE polymer with functionalized side chains was obtained by polymerizing monomers **3** and **4** via the Sonogashira reaction. The polymerization was carried out in THF with Pd(PPh₃)₄ as catalyst, Et₃N as base, and CuI as cocatalyst (Scheme 3). Iodobenzene was used as a chain stopper to limit the molar mass in order to obtain soluble material and a fixed DP of 30 units.^{28–30} GPC analysis results in an \bar{M}_n value of 11.1 kg/mol and a dispersity of 1.4. The higher dispersity compared to P3HT can be explained to the step-growth polymerization mechanism.

To obtain the polymer with terminal azide groups in the side chains, two postpolymerization reactions were performed. First, the alcohol groups were converted to better leaving groups, i.e., tosyl groups, which were subsequently converted to azide groups by reaction with sodium azide in the presence of 18-crown-6 (Scheme 4).^{31–35}

¹H NMR spectroscopy was used to monitor these postpolymerization transformations (Figure 2). This reveals that the reactions occurred quantitatively.

For grafting P3HT to the PPE backbone the CuAAC click reaction was used with CuBr/PMDTA as catalyst system (Scheme 5). The high yields of this reaction should allow a high control over grafting density and enable us to obtain high

Scheme 3. Synthesis of Polymer P2



Scheme 4. Synthesis of Polymer P4 via Two Postpolymerization Reactions

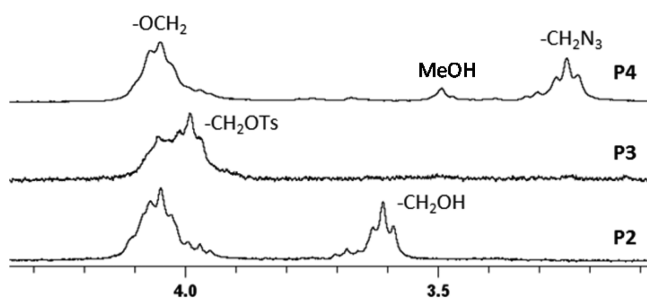
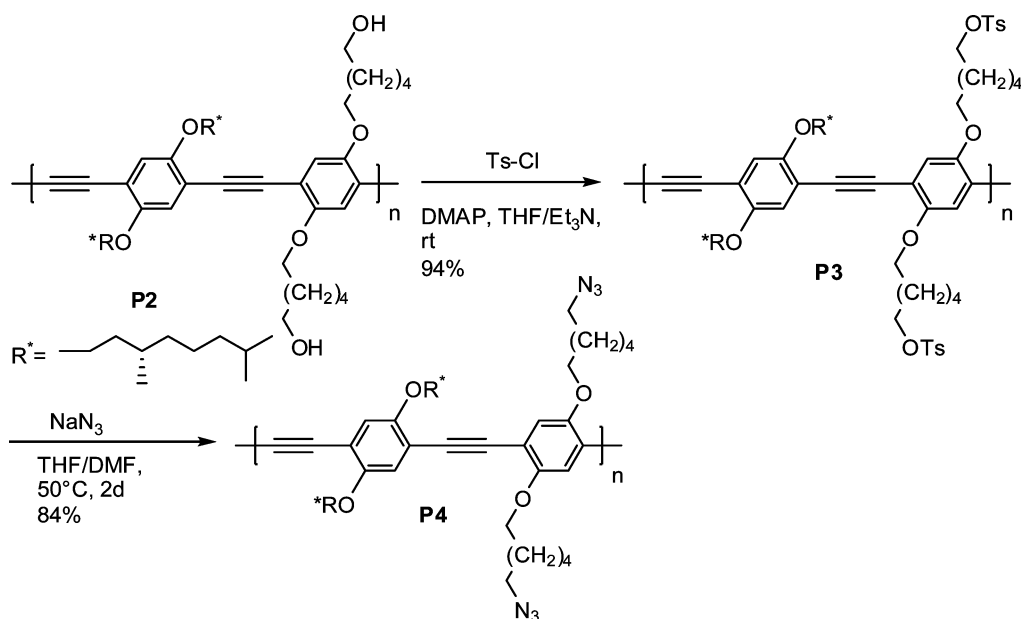


Figure 2. ^1H NMR signals of $-\text{OCH}_2$ and $-\text{CH}_2$ groups next to the functional end group of the side chains of P2, P3, and P4.

degrees of functionalization. This reaction is often used to synthesize graft copolymers by the “grafting to” method.^{36–39}

By adjusting the ratio between P1 and P4, percentages of functionalization of 10 (P5), 25 (P6), 50 (P7), and 100 (P8) were aimed for (see Supporting Information). Note that gel formation could have been anticipated (especially for P8) as some dicapped P3HT is present. However, this is not observed.

GPC and ^1H NMR of the Graft Copolymers. To remove residual homopolymers, the graft copolymers were purified by preparative GPC. The purified graft copolymers were analyzed by GPC; chromatograms and corresponding \bar{M}_n and dispersity values are displayed in Figure 3 and Table 1, respectively. There

is a clear increase in molar mass upon increasing the ratio of P1 to P4. The dispersities of the graft copolymers have the same value due to purification by preparative GPC. Consequently, a study of the influence of the grafting degrees on the properties can be considered valid.

Since the correction factor for the real \bar{M}_n and \bar{M}_w measured by GPC for both P3HT and PPE are known and the amount of P3HT and PPE in the graft copolymers is known as well (from ^1H NMR), the real \bar{M}_n of the graft copolymers can be calculated. This reveals that GPC overestimates \bar{M}_n by a factor of 2.

In order to check if the aimed degrees of functionalization correspond to what was aimed for, a ^1H NMR analysis was performed. Already at first glance, it is obvious that the peaks corresponding to P3HT increase dramatically (Figure 4).

To have a precise determination of the grafting percentages, the integration values of the $-\text{OCH}_2$ peaks (a) and the N_3-CH_2 protons (b) of PPE were determined (Figure 5).

The grafting percentage is then calculated by the following formula:

$$\text{grafting \%} = 1 - \frac{\text{no. of nonreacted azide functions}}{\text{no. of initial azide functions}} \\ \times 100\% = 1 - \frac{b/2}{a/4} \times 100\%$$

Scheme 5. Synthesis of the Four Graft-Copolymers P5–P8

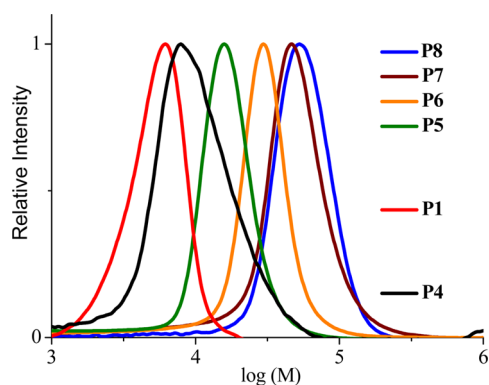
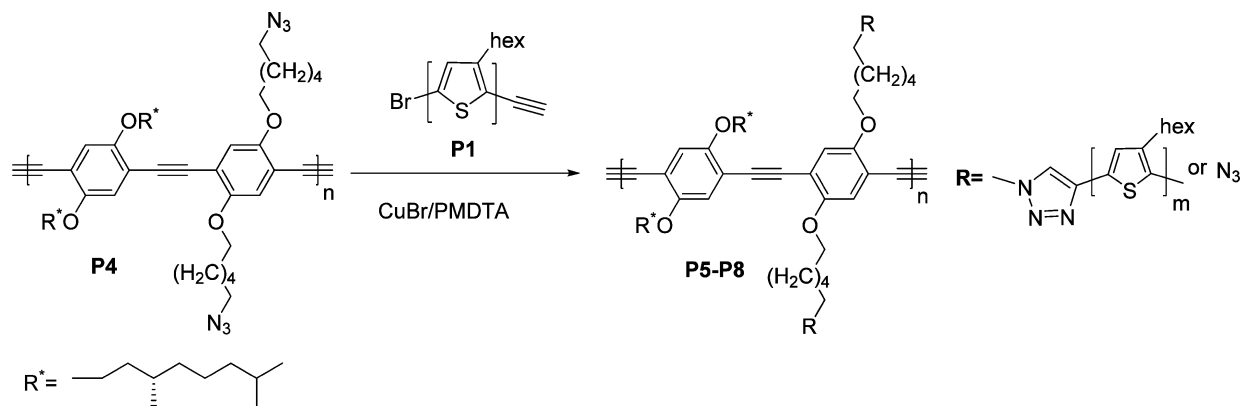


Figure 3. Chromatograms of homopolymers P1 and P4 and of the graft copolymers P5–P8.

While aimed for 10, 25, 50, and 100%, values of 10, 24, 38, and 50% were achieved (Table 1). It is clear that the deviation increases with increasing degrees of functionalization. This can be explained by the increasing steric hindrance, which is in general the limiting factor for the “grafting to” method. Note that this nicely correlates with $[d/(20 \cdot 2)]/(a/4)$ (Table 1). This formula corresponds with the calculations of grafting % using the α -CH₂ protons of the P3HT side chains and assuming a degree of polymerization of 20. This result suggests that the degree of polymerization is indeed close to 20.

UV–Vis Spectroscopy. UV–vis experiments were performed on both homopolymers (P1 and P4) and the four graft copolymers (P5–P8). For all of them ten solutions were made with an increasing amount of methanol in comparison to chloroform (Supporting Information, S11–16). In pure chloroform both P3HT and PPE absorb around 440 nm, although the P3HT absorption is characterized by a broader

peak.⁴⁰ Upon increasing the methanol content the absorption band is red-shifted for P3HT due to aggregation. This occurs starting from 30% MeOH. For PPE, this red-shift is not observed; aggregation is only visible by the appearance of an extra peak around 480 nm.⁴¹ Aggregation occurs starting from 60% MeOH (see Supporting Information). From the spectra of the graft copolymers in 90% MeOH a clear contribution of PPE is still visible for P5 (Figure 6). Also, for P6 the characteristic band at 480 nm of PPE can still be observed. However, for P7 and P8 the UV–vis spectra are nearly identical to the P3HT homopolymer P1, although the fine structure is somewhat less defined. This is in line with the fact that the P3HT content increases dramatically from P5 to P8.

Also, spectra in 90% MeOH were simulated using the spectra of the corresponding homopolymers and their respective mass fraction in order to investigate the influence of the backbone and side chains on their aggregation (Figure 7). For this simulation, the behavior of the graft copolymers was modeled as a linear combination of both homopolymers. The fraction of the two polymers contributing to the spectrum of the graft copolymers was calculated using the mass fraction determined from ¹H NMR. If the two polymers would not influence each other, the simulated and experimental spectra would coincide. However, the peak around 600 nm, originating from aggregated P3HT, is less pronounced in the experimental spectra compared to the simulated spectra for P6–P8. This less pronounced fine structure demonstrates that the stacking of the P3HT in the graft copolymers is complicated due to their covalent bond to the PPE backbone. Note that UV–vis cannot provide much information on the PPE aggregation, as the UV–vis spectrum is rather insensitive for self-assembly and the smaller fraction of PPE present. In summary, the UV–vis study indicates that the PPE compromises the self-assembly of the P3HT.

Table 1. \bar{M}_n and \bar{D} Values of Homopolymers P1 and P4 and of the Graft Copolymers P5–P8 and Aimed vs Calculated Grafting Percentages

polymer	\bar{M}_n (kg/mol)	\bar{D}	aimed grafting (%)	grafting % (NMR)	
				$1 - [(b/2)/(a/4)] \times 100\%$	$[d/(20 \cdot 2)]/(a/4) \times 100\%$
P1	4.4	1.2			
P4	11.1	1.4			
P5	15.8	1.2	10	10	11
P6	27.4	1.2	25	24	24
P7	45.9	1.2	50	38	37
P8	50.3	1.2	100	50	50

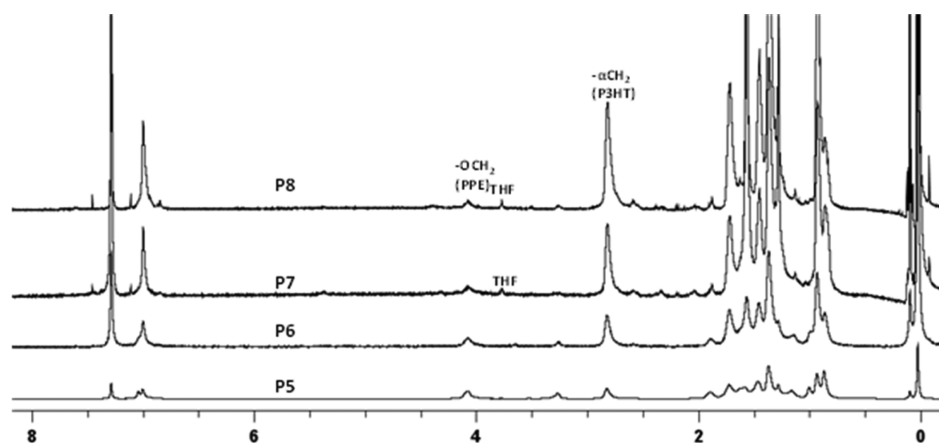


Figure 4. ^1H NMR spectra of graft copolymers P5–P8.

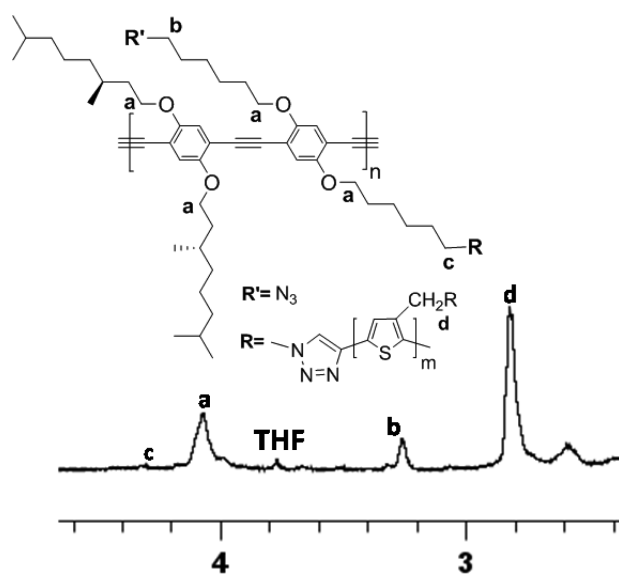


Figure 5. ^1H NMR spectrum of P6 in the region 2.5–4.5 ppm.

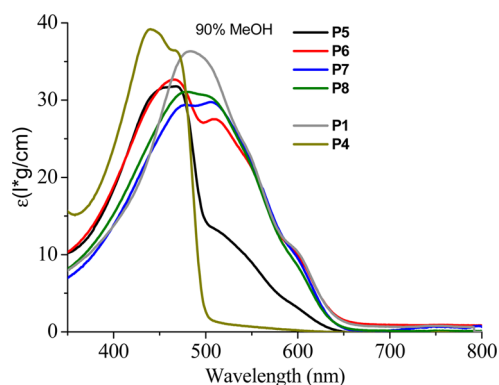


Figure 6. UV–vis spectra of homopolymers P1 and P4 and graft copolymers P5–P8 in MeOH/ CHCl_3 (9/1). $c_{\text{P1}} = 0.026$ g/L; $c_{\text{P4}} = 0.026$ g/L; $c_{\text{P5}} = 0.018$ g/L; $c_{\text{P6}} = 0.019$ g/L; $c_{\text{P7}} = 0.020$ g/L; $c_{\text{P8}} = 0.032$ g/L.

CD Spectroscopy. Also, CD spectra for 90% MeOH solutions of homopolymers and graft copolymers were obtained (Figure 8). From the self-assembly of the homopolymers, it is clear that in these conditions both the P3HT and PPE self-assemble—if this would be possible. The PPE backbone

contains chiral side chains, allowing chiral stacking, resulting in a CD signal. Such signal was also observed for the homopolymer. Naturally, since the P3HT is achiral, no CD is observed.

For the graft copolymers, only a Cotton effect is observed for P5, the graft copolymer with the lowest grafting density. The region of the Cotton effect is the same as in P4, showing that the Cotton effect originates from the PPE. The other polymers do not show any CD, pointing at the absence of chiral self-assembly. Interestingly, the CD effect of P5 changes sign compared to homopolymer P4. This rules out that the effect originates from some PPE that does not contain any P3HT, as this would result in a smaller, positive Cotton effect. This also shows that the P3HT influences the (chiral) self-assembly of the PPE. Combined with the UV–vis results, these data show that the PPE and P3HT influence each other's self-assembly and that the chiroptical behavior of these conjugated graft copolymers is no simple superposition of the two polymers.

Atomic Force Microscopy (AFM). Figures 9a,b illustrate the typical topographic Tapping Mode AFM images of thin deposits of P7 and P8 (prepared from 0.01–0.1 mg/mL solutions). Compared to what is generally observed for linear conjugated polymers,^{42–45} here the polymer chains are not all organized as fibrillary assemblies.

As suspected from the spectroscopic data, it appears that upon solvent evaporation the polymer chains do not form organized assemblies; instead, they tend to collapse into round-shaped objects ranging from about 20 to 100 nm in diameter, whatever the solvent used (THF or chloroform). The smallest objects may contain only few polymer chains while the larger ones are made of more chains. The aggregate size mainly depends on the solvent evaporation kinetics and the initial polymer concentration (larger aggregates are observed when using more concentrated polymer solutions). This lack of organization is most probably due to the fact that the PPE segments are far from each other because of the presence of the P3HT side chains, which prevents any π – π stacking and long-range assembly of the conjugated backbone. For similar reasons, the P3HT branches cannot interact to form fibrils. For the P8 graft polymer, and whatever the solvent, the morphology is also showing nonorganized round-shaped objects despite the higher grafting density.

Differential Scanning Calorimetry (DSC). DSC measurements were performed on the polymer powders (Supporting Information, S16). P1 shows a clear melting peak at 178 °C.

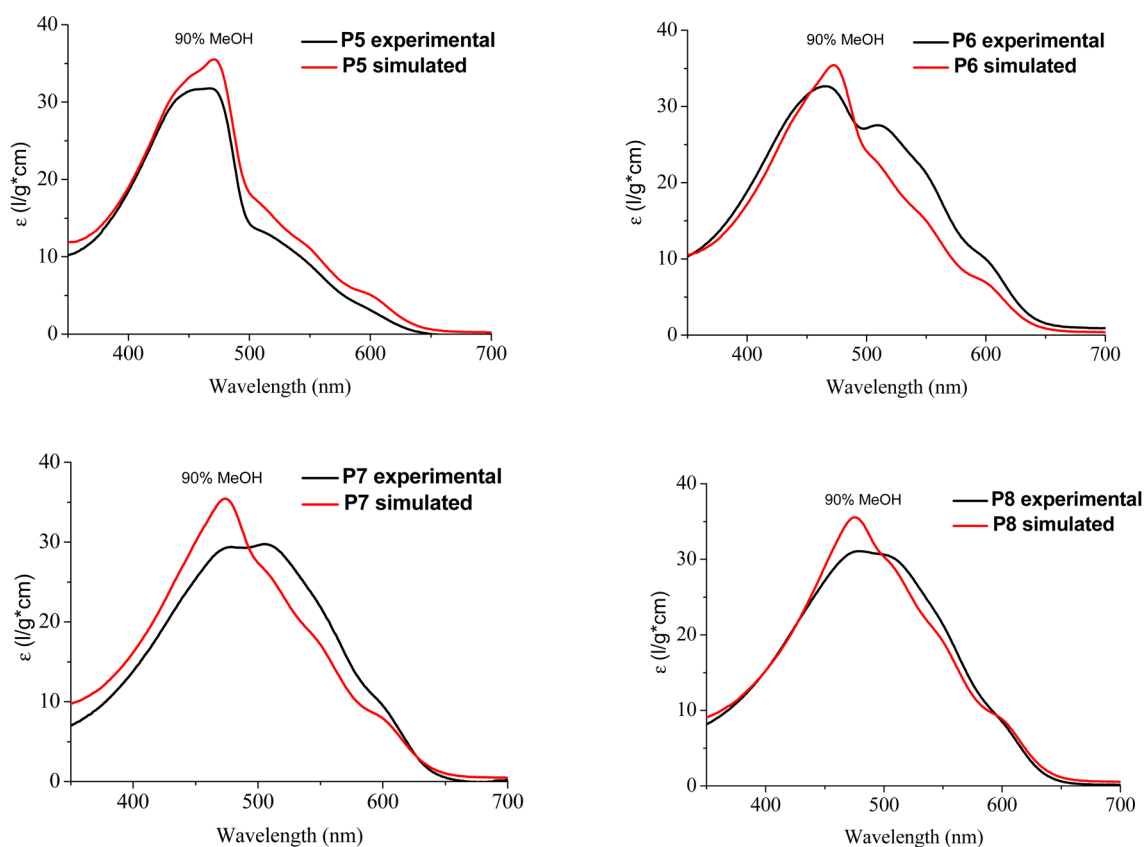


Figure 7. Experimental vs simulated UV-vis of graft copolymers **P5–P8** in MeOH/CHCl₃ (9/1).

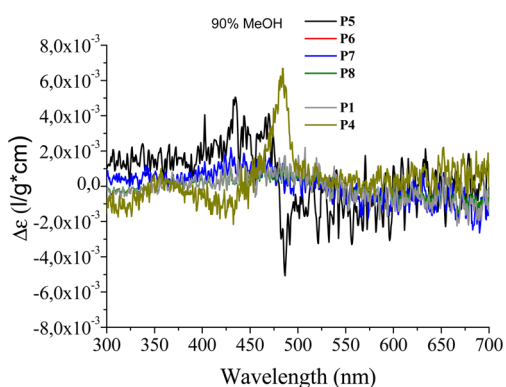


Figure 8. CD spectra of graft copolymers **P5–P8** in MeOH/CHCl₃ (9/1). $c_{P1} = 0.026$ g/L; $c_{P4} = 0.026$ g/L; $c_{P5} = 0.018$ g/L; $c_{P6} = 0.019$ g/L; $c_{P7} = 0.020$ g/L; $c_{P8} = 0.032$ g/L.

Also, for **P8** an onset of a melting peak at 138 °C is observed. Besides the lower melting temperature compared to **P1**, also the melting enthalpy dropped from 5 J/g to 3 mJ/g. For all other graft copolymers no melting peaks were observed. This result, in accordance with the UV-vis and AFM observations, indicates that the presence of a small amount of PPE is sufficient to disrupt the crystallization of poly(3-hexylthiophene).

Fluorescence Spectroscopy. Fluorescence was measured for solutions of the polymers in pure chloroform at an excitation wavelength of 440 nm. The $\lambda_{\max,em}$ for the PPE backbone is around 473 nm, while that of the P3HT side chains is around 574 nm (Figure 10). Although P3HT and PPE absorb at the same wavelength region around 440 nm, they

emit at different wavelengths due to a difference in the Stokes shift. A first look at the fluorescence spectra shows a dramatic decrease of the fluorescence of the PPE backbone for increasing grafting densities. The amount of quenching was calculated (see Supporting Information). As the fluorescence and the extinction coefficient of the homopolymers and the mass fraction of PPE and P3HT are known, energy transfer from the PPE backbone to the P3HT side chains can be calculated. An enormous degree of quenching is found for the fluorescence of the PPE backbone (Table 2). The smaller quenching for **P5** in comparison to the other graft copolymers may be due to the presence of a very small amount of homopolymer **P4**. Indeed, while very small amounts of homopolymer (a few percent) are not visible by GPC or CD, this amount can already result in a significant fluorescence.

CONCLUSION

We report the first use of the “grafting to” method for the synthesis of conjugated graft copolymers with a backbone and side chains of different chemical nature (PPE and P3HT, respectively). To achieve this goal, the CuAAC click reaction was used to click acetylene end-functionalized P3HT to azide-functionalized PPE. GPC demonstrates the synthesis of graft copolymers with an increasing grafting density. Using ¹H NMR analysis, grafting percentages of 10, 24, 38, and 50% were calculated for **P5–P8**. This is close to what was aimed for except for **P8**. The (chiral) self-assembly was studied by means of UV-vis and CD spectroscopy, AFM, and DSC. These techniques showed that the aggregation behavior is not a linear combination of backbone and side chains independent of each other. The aggregation of the backbone as well as the side

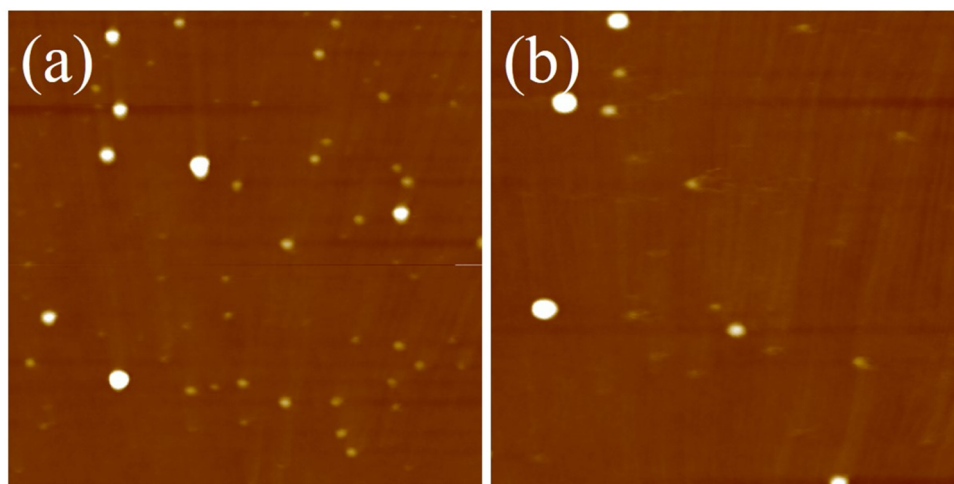


Figure 9. Tapping mode AFM height images ($5.0 \mu\text{m} \times 5.0 \mu\text{m}$) of (a) P7 and (b) P8. The Z-range is 50 nm. The solvent was THF for P7 and chloroform for P8.

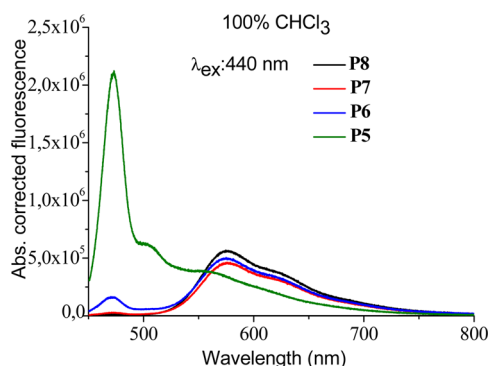


Figure 10. Fluorescence spectra of graft copolymers P5–P8 in CHCl_3 , $c_{\text{P1}} = 0.0026 \text{ g/L}$; $c_{\text{P4}} = 0.0026 \text{ g/L}$; $c_{\text{P5}} = 0.0018 \text{ g/L}$; $c_{\text{P6}} = 0.0019 \text{ g/L}$; $c_{\text{P7}} = 0.0020 \text{ g/L}$; $c_{\text{P8}} = 0.0032 \text{ g/L}$.

Table 2. Calculated Percentages of Energy Transfer

graft copolymer	quenching PPE
P5	−6
P6	−96
P7	−99
P8	−99

chains is compromised by the covalent bonding to each other. AFM data indicate that there is no self-assembly of the polymer chains in the solid state. This is indicated by a disappearance of the melting peak in DSC, the disappearance of fine structure in the UV–vis spectra, and the disappearance of a chiral response of the backbone in the CD spectra. Quenching of the fluorescence of PPE was observed even when the ratio of PPE/P3HT is small.

■ ASSOCIATED CONTENT

● Supporting Information

The Supporting Information is available free of charge on the ACS Publications website at DOI: 10.1021/acs.macromol.5b01830.

Synthesis of monomer, linear homopolymers, and graft copolymers; ^1H NMR, UV–vis, CD, and fluorescence spectra of the linear polymers (P1 and P4) and the graft copolymers (P5–P8); MALDI-ToF spectrum of P1; a

comparison between the experimental and simulated spectra of the graft copolymers (P5–P8) in 90% MeOH; DSC thermograms of P1 and graft copolymers P5–P8 (PDF)

■ AUTHOR INFORMATION

Corresponding Author

*(G.K.) E-mail: guy.koeckelberghs@chem.kuleuven.be.

Notes

The authors declare no competing financial interest. Ph.L. is F.R.S.-FNRS Senior Research Associate.

■ ACKNOWLEDGMENTS

We are grateful to the Onderzoeksfonds K.U. Leuven/Research Fund K.U. Leuven and the Fund for Scientific Research (FWO-Vlaanderen) for financial support. J.S. is grateful to IWT for a doctoral fellowship. Research in Mons is supported by the Science Policy Office of the Belgian Federal Government (PAI 7/5), the European Commission/Région Wallonne FEDER program, and the “Fonds National pour la Recherche Scientifique” (FRS-FNRS). The MONS laboratory is grateful to the “Fonds National pour la Recherche Scientifique” (FRS-FNRS) for financial support for the acquisition of the Waters QToF Premier mass spectrometer and for continuing support.

■ ABBREVIATIONS

PPE, poly(phenyleneethynylene); P3HT, poly(3-hexylthiophene); PMDTA, N,N,N',N'',N''' -pentamethyldiethylenetriamine; CD, chiral dichroism; DSC, density scanning calorimetry; GPC, gel permeation chromatography; MALDI-ToF, matrix assisted laser desorption ionization–time of flight; GRIM, Grignard methatesis; KTCP, Kumada catalyst transfer polymerization; CuAAC, copper assisted azide click chemistry; \bar{M}_n , number-average molecular weight; DP, degree of polymerization; AFM, atomic force microscopy.

■ REFERENCES

- (1) Feng, C.; Li, Y.; Yang, D.; Hu, J.; Zhang, X.; Huang, X. *Chem. Soc. Rev.* **2011**, *40*, 1282–1295.
- (2) Runge, M. B.; Bowden, N. B. *J. Am. Chem. Soc.* **2007**, *129*, 10551–10560.
- (3) Facchetti, A. *Chem. Mater.* **2011**, *23*, 733–758.

- (4) Zhan, X.; Zhu, D. *Polym. Chem.* **2010**, *1*, 409.
- (5) Friend, R. H.; Gymer, R. W.; Holmes, A. B.; Burroughes, J. H.; Marks, R. N.; Taliani, C.; Bradley, D. D. C.; Dos Santos, D. A.; Bredas, J. L.; Logdlund, M.; Salaneck, W. R. *Nature* **1999**, *397*, 121–128.
- (6) Sirringhaus, H.; Brown, P. J.; Friend, R. H.; Nielsen, M. M.; Bechgaard, K.; Langeveld-Voss, B. M. W.; Spiering, A. J. H.; Janssen, R. A. J.; Meijer, E. W.; Herwig, P.; de Leeuw, D. M. *Nature* **1999**, *401*, 685–688.
- (7) Steverlynck, J.; Leysen, P.; Koeckelberghs, G. *J. Polym. Sci., Part A: Polym. Chem.* **2015**, *53*, 79–84.
- (8) Shen, J.; Masaoka, H.; Tsuchiya, K.; Ogino, K. *Polym. J.* **2008**, *40*, 421–427.
- (9) Pu, K.-Y.; Chen, Y.; Qi, X.-Y.; Qin, C.-Y.; Chen, Q.-Q.; Wang, H.-Y.; Deng, Y.; Fan, Q.-L.; Huang, Y.-Q.; Liu, S.-J.; Wei, W.; Peng, B.; Huang, W. *J. Polym. Sci., Part A: Polym. Chem.* **2007**, *45*, 3776–3787.
- (10) Wang, J.; Lu, C.; Mizobe, T.; Ueda, M.; Chen, W.-C.; Higashihara, T. *Macromolecules* **2013**, *46*, 1783–1793.
- (11) Zeigler, D. F.; Mazzio, K. A.; Luscombe, C. K. *Macromolecules* **2014**, *47*, 5019–5028.
- (12) Langeveld-Voss, B. M. W.; Beljonne, D.; Shuai, Z.; Janssen, R. A. J.; Meskers, S. C. J.; Meijer, E. W.; Brédas, J.-L. *Adv. Mater.* **1998**, *10*, 1343–1348.
- (13) Van den Bergh, K.; Cosemans, I.; Verbiest, T.; Koeckelberghs, G. *Macromolecules* **2010**, *43*, 3794–3800.
- (14) Atkins, K. M.; Martínez, F. M.; Nazemi, A.; Scholl, T. J.; Gillies, E. R. *Can. J. Chem.* **2011**, *89*, 47–56.
- (15) Ma, Z.; Li, Y.-B.; Deng, K.; Lei, S.-B.; Wang, Y.-Y.; Wang, P.; Yang, Y.-L.; Wang, C.; Huang, W. *J. Phys. Chem. C* **2010**, *114*, 11460–11465.
- (16) Makal, T. A.; Wang, X.; Zhou, H. C. *Cryst. Growth Des.* **2013**, *13*, 4760–4768.
- (17) Wariishi, K.; Morishima, S. I.; Inagaki, Y. *Org. Process Res. Dev.* **2003**, *7*, 98–100.
- (18) Norris, B. N.; Pan, T.; Meyer, T. Y. *Org. Lett.* **2010**, *12*, 5514–5517.
- (19) Li, Z.; Ono, R. J.; Wu, Z.-Q.; Bielawski, C. W. *Chem. Commun.* **2011**, *47*, 197–199.
- (20) Urien, M.; Erothu, H.; Cloutet, E.; Hiorns, R. C.; Vignau, L.; Cramail, H. *Macromolecules* **2008**, *41*, 7033–7040.
- (21) Pang, X.; Zhao, L.; Feng, C.; Wu, R.; Ma, H.; Lin, Z. *Polym. Chem.* **2013**, *4*, 2025.
- (22) Tao, Y.; McCulloch, B.; Kim, S.; Segalman, R. A. *Soft Matter* **2009**, *5*, 4219.
- (23) De Winter, J.; Deshayes, G.; Boon, F.; Coulembier, O.; Dubois, P.; Gerbaux, P. *J. Mass Spectrom.* **2011**, *46*, 237–246.
- (24) Liu, J.; Loewe, R. S.; McCullough, R. D. *Macromolecules* **1999**, *32*, 5777–5785.
- (25) Verswyvel, M.; Monnaie, F.; Koeckelberghs, G. *Macromolecules* **2011**, *44*, 9489–9498.
- (26) Lee, J. K.; Ko, S.; Bao, Z. *Macromol. Rapid Commun.* **2012**, *33*, 938–942.
- (27) Wong, M.; Hollinger, J.; Kozycz, L. M.; McCormick, T. M.; Lu, Y.; Burns, D. C.; Seferos, D. S. *ACS Macro Lett.* **2012**, *1*, 1266–1269.
- (28) Bunz, U. H. *Chem. Rev.* **2000**, *100*, 1605–1644.
- (29) Palmans, A. R. A.; Smith, P.; Weder, C. *Macromolecules* **1999**, *32*, 4677–4685.
- (30) Bunz, U. H. F. *Macromol. Rapid Commun.* **2009**, *30*, 772–805.
- (31) Varma, R. S.; Naicker, K. P.; Aschberger, J. *Synth. Commun.* **1999**, *29*, 2823–2830.
- (32) Mantovani, G.; Ladmiral, V.; Tao, L.; Haddleton, D. M. *Chem. Commun.* **2005**, *16*, 2089–2091.
- (33) Liu, X.; Fan, Q.; Huang, W. *Biosens. Bioelectron.* **2011**, *26*, 2154–2164.
- (34) Yuan, H.; Liu, Z.; Liu, L.; Lv, F.; Wang, Y.; Wang, S. *Adv. Mater.* **2014**, *26*, 4333–4338.
- (35) Englert, B. C.; Bakbak, S.; Bunz, U. H. F. *Macromolecules* **2005**, *38*, 5868–5877.
- (36) Barner-Kowollik, C.; Du Prez, F. E.; Espeel, P.; Hawker, C. J.; Junkers, T.; Schlaad, H.; Van Camp, W. *Angew. Chem., Int. Ed.* **2011**, *50*, 60–62.
- (37) Fournier, D.; Hoogenboom, R.; Schubert, U. S. *Chem. Soc. Rev.* **2007**, *36*, 1369–1380.
- (38) Iha, R. K.; Wooley, K. L.; Nyström, A. M.; Burke, D. J.; Kade, M. J.; Hawker, C. J. *Chem. Rev.* **2009**, *109*, 5620–5686.
- (39) Bunz, U. *Synlett* **2013**, *24*, 1899–1909.
- (40) *Chromogenic Phenomena in Polymers*; Jenekhe, S. A., Kiserow, D. J., Eds.; ACS Symposium Series; American Chemical Society: Washington, DC, 2004; Vol. 888.
- (41) Halkyard, C. E.; Rampey, M. E.; Kloppenburg, L.; Studer-Martinez, S. L.; Bunz, U. H. F. *Macromolecules* **1998**, *31*, 8655–8659.
- (42) Leclère, P.; Hennebicq, E.; Calderone, A.; Brocorens, P.; Grimdsdale, A.; Müllen, K.; Brédas, J.; Lazzaroni, R. *Prog. Polym. Sci.* **2003**, *28*, 55–81.
- (43) Leclère, P.; Surin, M.; Viville, P.; Lazzaroni, R.; Kilbinger, A. F. M.; Henze, O.; Feast, W. J.; Cavallini, M.; Biscarini, F.; Schenning, A. P. H. J.; Meijer, E. W. *Chem. Mater.* **2004**, *16*, 4452–4466.
- (44) Willot, P.; Steverlynck, J.; Moerman, D.; Leclère, P.; Lazzaroni, R.; Koeckelberghs, G. *Polym. Chem.* **2013**, *4*, 2662–2671.
- (45) Willot, P.; Teyssandier, J.; Dujardin, W.; Adisoejoso, J.; De Feyter, S.; Moerman, D.; Leclère, P.; Lazzaroni, R.; Koeckelberghs, G. *RSC Adv.* **2015**, *5*, 8721–8726.